Fabricating Micro-channels using 3D Printing and Infiltration

Isa Kohls

A thesis submitted to the faculty of
Brigham Young University
in partial fulfillment of the requirements for the degree of

Bachelor of Science

Kent Gee, Chair
Robert Davis

Department of Physics and Astronomy

Brigham Young University

ABSTRACT

Gas chromatography (GC) is a technique used to separate and identify a wide range of volatile and semi-volatile compounds by sending a sample of gas through a long channel. A long channel is required for high resolution but makes the system slow and bulky. A high-resolution chromatograph with a shorter channel can theoretically be achieved by introducing a thermal gradient. This would decrease processing time and increase portability. We explore the feasibility of creating a long, narrow, sealed channel by binder jet 3D printing stainless steel powder and subsequently infiltrating with bronze. The purpose of the infiltration was to fill the pores within the stainless-steel matrix, but this process risked filling or blocking the channels necessary for gas flow in the GC system. Various designs and processes were adjusted to improve channel quality. Design requirements included ensuring printer powder removal, connections between sections of channel, directed infiltrant overflow, and imaging reliability. By milling the channeled blocks, we could qualitatively evaluate the porosity of the blocks as well as any blockage of the channels. We conclude that 3D printing and infiltration is a viable method to make channels suitable for micro-GC, but requires further research.

Keywords: additive manufacturing, chromatography, infiltration

Acknowledgments

I would like to thank Dr. Robert Davis, Dr. Richard Vanfleet, Dr. Brian D. Jensen, Dr. Nathan Crane, Henry Davis, James Harkness, and Collin Davis for the ample help they gave.

I would also like to thank BYU undergraduate mentorship funding.

Table of Contents

Table of Figures

Chapter 1 INTRODUCTION

1.1 Gas Chromatography

Gas chromatography (GC) is a technique that separates and identifies a wide range of volatile and semi-volatile compounds. It has a variety of applications including testing for pollution, biofuel research, natural gas quality verification, detection of illicit drugs, work safety, arson investigation, paint chip analysis, and toxicology cases. GC systems are accurate and reliable but are limited in their use due to their large size and high energy consumption. The bulk is an inherent quality of how such systems function.

A general schematic of a GC system is shown in figure 1.1. The sample gas and carrier gas flow through a column coated with a sticky material called stationary phase. Different compounds become trapped in the stationary phase for different amounts of time and thus go through the channel at different rates. The mixture needs time and space to separate into its distinct components, so the length of the column through which the gas travels is a principal contributor to accuracy and resolution. Though necessary in traditional systems, a long column makes the system large and slow. Their use is limited to labs. GC is versatile enough to find uses in many more applications. Portable machines could be used to treat people in ambulances, to test toxicity/pollution on-site, to test ground water contamination, to advance space exploration, and to contribute to other various time-sensitive applications.

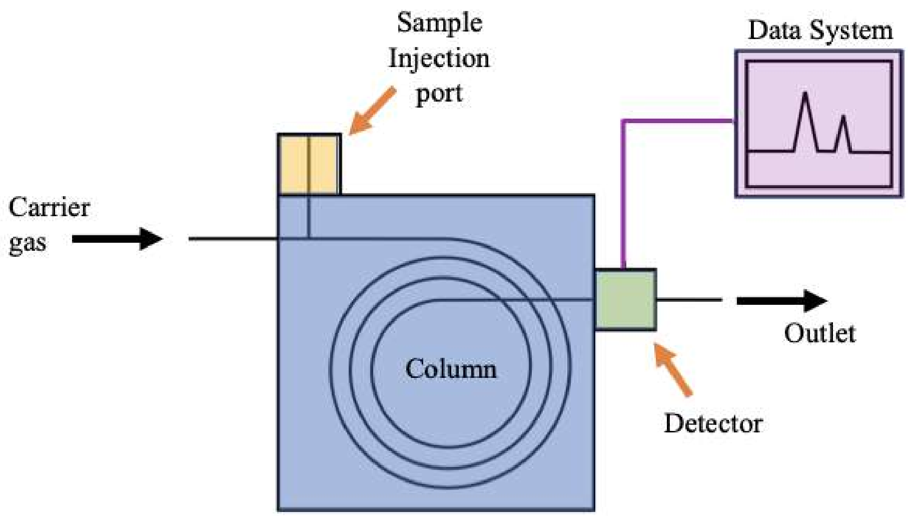

Figure 1.1 *Diagram of a GC system. An inert carrier gas pushes the sample gas through the column. The column is coated with stationary phase that interacts with different molecules nearly uniquely. Some molecules become trapped in the stationary phase often, and for long periods of time each instance they become trapped. These molecules come out of the channel later than those that hardly interact with the stationary phase at all. The gas thus separates into its various components. Each component is then detected and identified as it exits the column and enters the detector.*

1.2 Shorter Columns in Gas Chromatography

There are ways to utilize a shorter column while still maintaining high resolution. A temperature ramp potentially offers this capability [1]. One way to apply this technique includes making the channel out of a thermally conductive material. Micro-Gas Chromatography (μGC) systems typically use channels 1-3 m long while the standard GC uses channels typically 30-100 m long. This decrease in length is coupled with a decrease in diameter: 0.5 mm in μGC compared to 5 mm in traditional GC [2]. Mid-sized GC systems have been built, however the need for even more portable GC systems remains.

Most μGC channels are etched onto silicon wafers [2]. We chose to use 3D printing in our research instead because it allows more versatility in geometry. For example, channels can be built in three dimensions (opposed to the single plane of wafers) and the cross-sectional geometry can be rounded. Rounded channels reduce band broadening (making the channel more efficient) by avoiding the accumulation of the stationary phase at sharp corners (pooling) [3].

The goal of this research is to fabricate channels for use in a μGC system. To make this system with a resolution higher than other μGC systems, the channels must be made of a thermally conductive material to allow a thermal gradient. We have chosen to use binder jet 3D printing with stainless steel powder. The channels then undergo bronze infiltration to further improve desirable characteristics such as void filling (increased density), as discussed in section 2.4. Bronze infiltration of binder jet 3D printed ferrous powder has resulted in net-shape 98% dense objects [4].

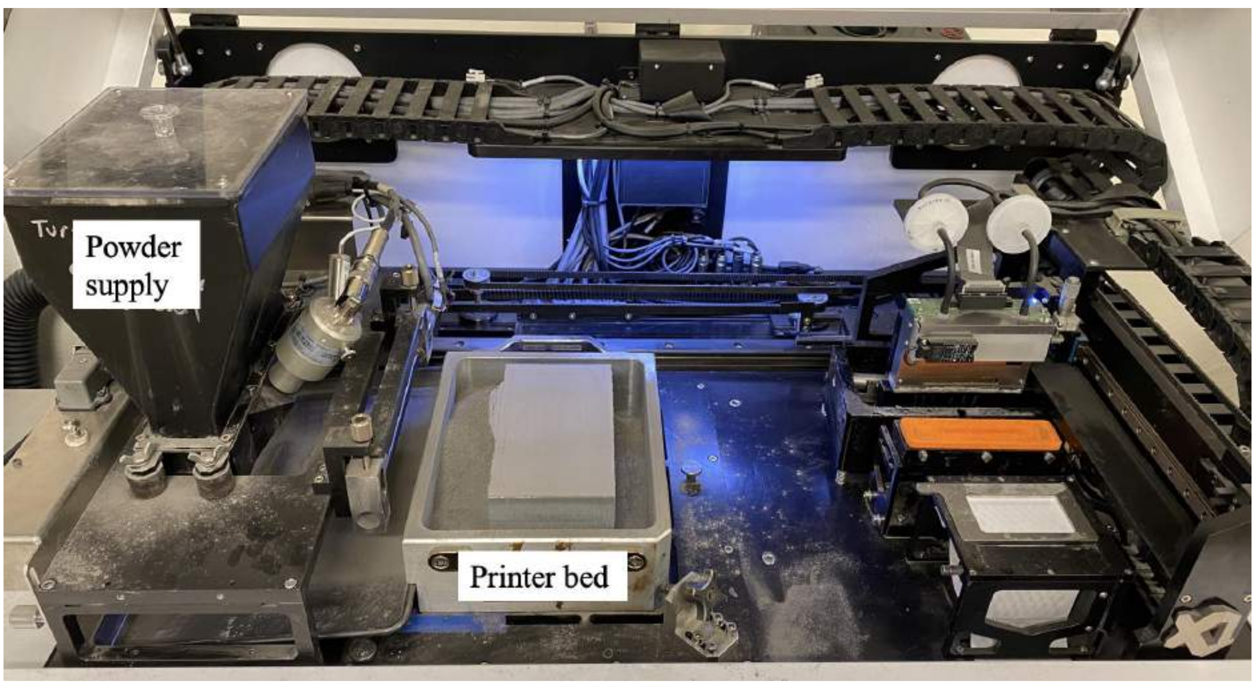

Figure 1.2 *A binder jet 3D printer. The ink jet head is very precise and small details can be printed. The head prints glue onto the printer bed in the desired design. The printer bed drops, and the roller spreads a thin layer of powder on top. The process repeats until the part is finished. The printer bed is placed in a furnace and the part is cured. Loose powder is removed, and the printed part is complete.*

1.3 Binder jet 3D printing

Additive manufacturing has greatly expanded manufacturing capabilities. Binder jet 3D printing, specifically offers rapid prototyping of small, precise, detailed parts made of metal. Our binder jet printer is shown in figure 1.2. Due to the imperfections of additive manufacturing, it is common to use other fabrication methods with it [5].

With this manufacturing method, we may be able to fabricate thermally conductive micro-channels for use in GC. The printing, sintering, and infiltrating processes are described in the methods section. Various design requirements set by μGC standards, printing limitations, and infiltration variability are also described. This project is a method-based project. The results are explored with an emphasis on the methods, and best methods of fabrication using our machines and resources are discussed. By qualitatively analyzing porosity, infiltrant overflow, and plate sealing, we conclude that 3D printing and infiltration micro-channels for GC offers potential, but more research is needed.

1.4 Other Applications of Micro-Channels

The methods to create μGC columns could be useful in other situations. Advances in gas chromatography can often be applied to liquid chromatography. As another example, these thermally conductive tubes could increase the heating/cooling efficiency of motors and other machines. The versatility of 3D printing combined with new understanding of the fabrication process may allow similar, more complicated micro-structures to be created in thermally conductive materials.

Chapter 2 METHODS

2.1.1 Binder Jet 3D Printing

Additive manufacturing allows rapid prototyping of precise custom parts made of a variety of materials. For our research we used a binder jet 3D printer with 316L stainless steel powder. We chose this metal due to its high availability, high thermal conductivity, and high melting point (this last characteristic becomes important in the infiltration process, explained in section 2.4).

GC columns have been made successfully from stainless steel [2]. Robust and inexpensive microchip columns 0.24 mm wide and 2.8 mm long were fabricated by wet etching on 0.5 mm thick stainless-steel plates [6]. We believe that 3D printing will allow the fabrication of even longer columns.

Binder jet printing is powder based. A roller spreads a layer of powder on the powder bed, then the printer head ejects binder (glue) in the desired design. A new layer of powder is spread, and the process repeats until the part is finished. The printing process in illustrated in figure 2.1. The part is then cured at 400 ^{o}C for over three hours and removed from the surrounding loose powder. Cured parts are fairly low density. Before sintering, the relative density of metallic parts created by binder jet printing is typically around 50–60% of the theoretical density of the material [7]. For our application, the highest performance of the printed parts would be achieved at, or close to, theoretical density.

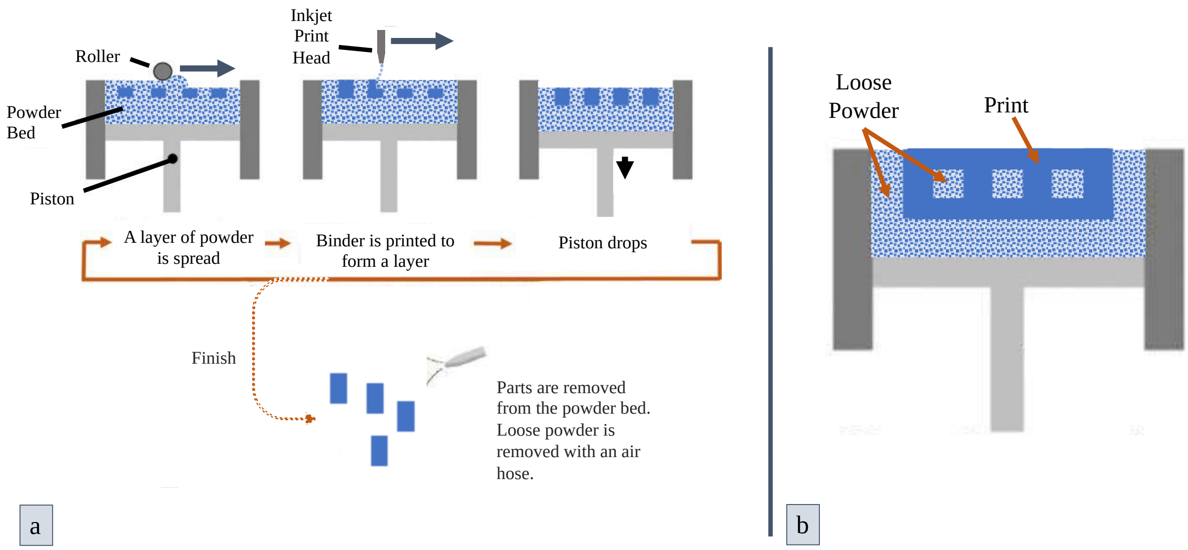

Figure 2.1 *Binder jet printing process (a) and printing an enclosed channel (b). Printing an enclosed channel is problematic because loose printer powder is difficult to remove from the part and clogs the enclosure.*

2.1.2 Design

The printing method has serious limitations. Binder jet printing cannot be used to make any sort of enclosed structure. After printing, the loose powder stays trapped in the encasing, often rendering the part useless. A single block with a long serpentine channel is not feasible because the loose powder would be trapped inside; the channel would be blocked and unusable.

To design around this, we printed plates with exposed channels designed to stack together. We used two distinct, but similar designs. The two designs had the same basic function with differences in dimensions and in their methods of dealing with excess bronze. The first design uses printed sacrificial structures in the form of slits and the second design uses a moat to accommodate a sacrificial powder.

A plate from the first (sacrificial structure) design is shown in figure 2.2a. The open face allowed channels to be cleared easily. Plates were 1 mm thick, with a base of 30 mm by 32 mm. A serpentine channel 50.5 cm long was printed as an indent 610 µm deep with a curved bottom.

After shrinkage from sintering, the channels measured to be about 500 μm in diameter, the larger end of standard μGC. A serpentine channel geometry was used because it has been shown to be more efficient in μGC [8].

The bottom plate was 4 mm thick and included an infiltrant holder. The design of a bottom plate is given in Figure 2.2b. Top and bottom plates were made with center holes to allow easier attachment to a ferrule, which then would connect to other apparatuses of the GC system.

The base and plates were designed to connect together to form one continuous channel, each plate alternating by a rotation of 180°. This stacking technique allowed fabrication of a channel longer than any single plate could fit. The layer above the channel acted as a lid, resulting in an extended hemispherical cross-sectional shape of the channel (figure 2.3). Each plate had ball-and-slot alignments to allow precise stacking (figure 2.4). Precise stacking is necessary for the vertical sections of channels between plates to connect adequately. A whole assembly of the first (sacrificial structure) design is shown in figure 2.5 with arrows to show where the channel connects between layers. More intermediate plates could be used, only two are shown here.

Small slits along the outsides of the plates served as sacrificial structures to hold bronze overflow, which will be further discussed in section 2.4. The structures were 1 mm deep and 0.15 mm wide with 0.10 mm gaps between them (figure 2.6).

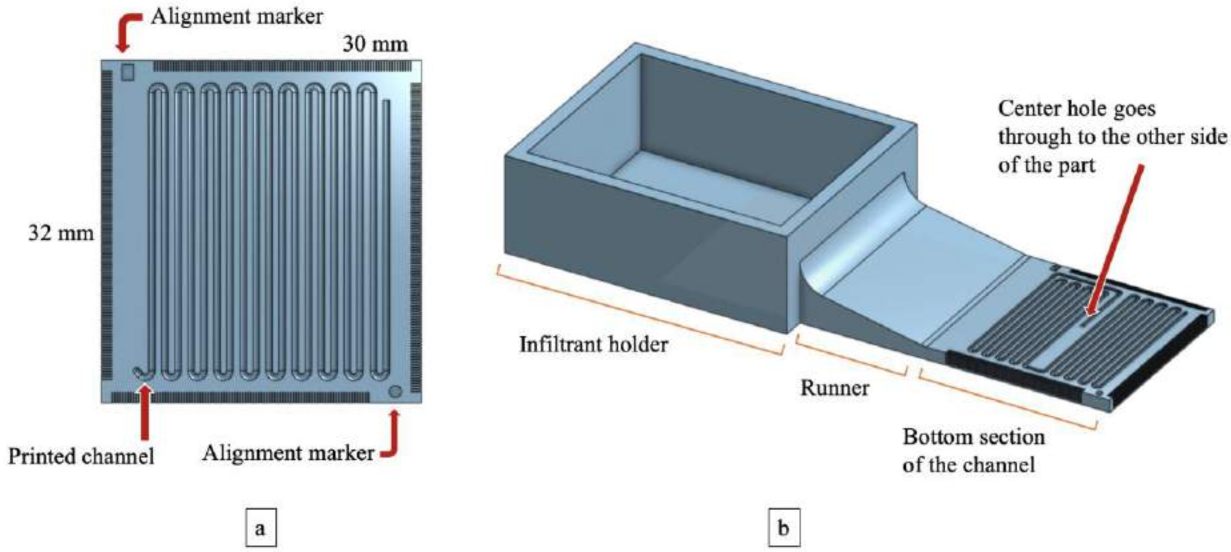

__Figure 2.2__ A typical plate in stackable assembly (a) and the bottom plate with a runner connecting to an infiltrant holder (b). The typical print dimensions of a plate are 1 mm x 30 mm x 32 mm with 50.5 cm of channel length. Alignment markers and vertical sections of the channels allow the block to stack together to create one long channel. Small slits around the edges serve to catch overflowing bronze during infiltration (see section 2.4). The top and bottom plates have channels that lead out of the center of the plates to allow easier ferrule attachment.

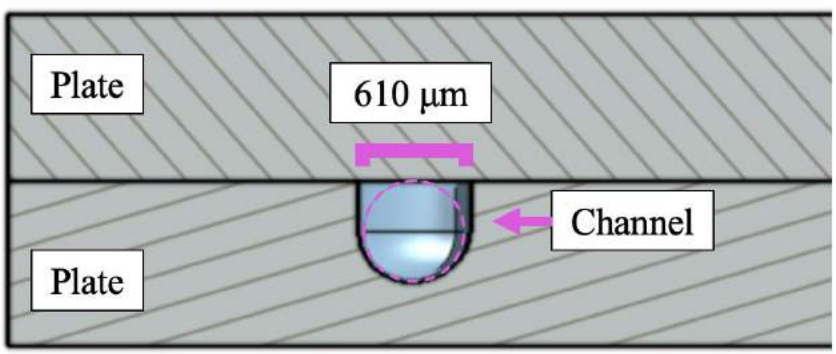

__Figure 2.3__ Side view of two plates, one on top of the other. The bottom plate has an open-faced printed channel while the top plate acts as a lid to enclose the channel. The channel is 610 µm deep and 610 µm wide with a hemispherical bottom. After sintering the channel diameter shrinks to about 500 µm.

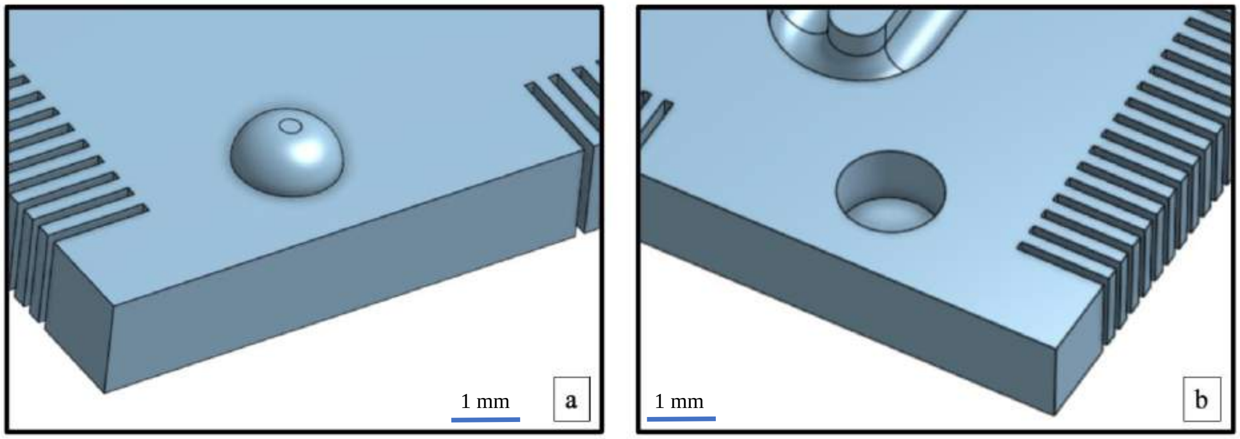

Figure 2.4 *Ball-and-slot alignment markings to allow precise stacking of the plates. There are two balls and two slots per plate. The balls are on the back of the plates while the slot in on the front with the channels. The circular alignment slot can be seen in the bottom right of the plate in figure 2.1a. A rectangular alignment slot is in the upper left corner of the same image.*

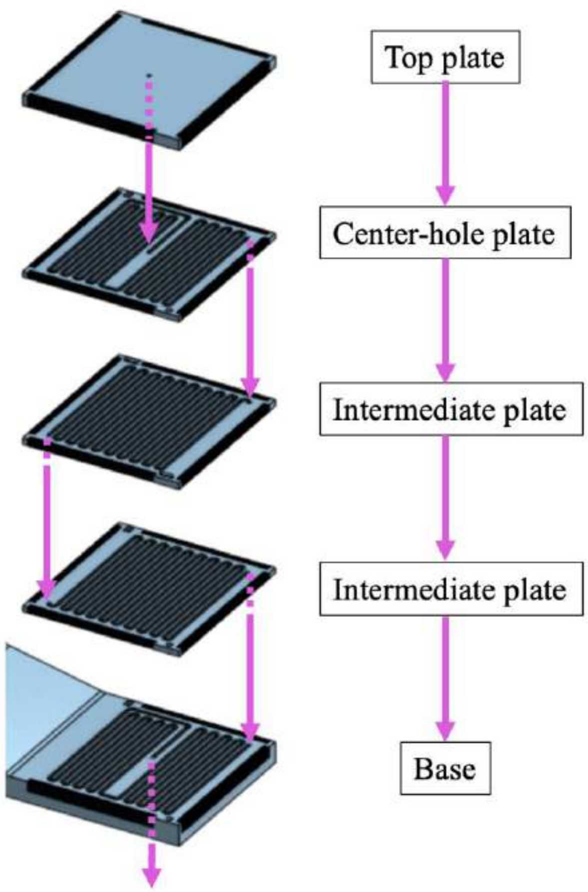

Figure 2.5 *Assembly of the stackable structure. The top plate and base use center exit holes to allow easier attachment to ferrules (not shown). Intermediate plates are identical to each other, only alternating by 180 degrees when stacking. More intermediate plates may be used than are shown here. The hypothetical flow of gas is illustrated by the arrows.*

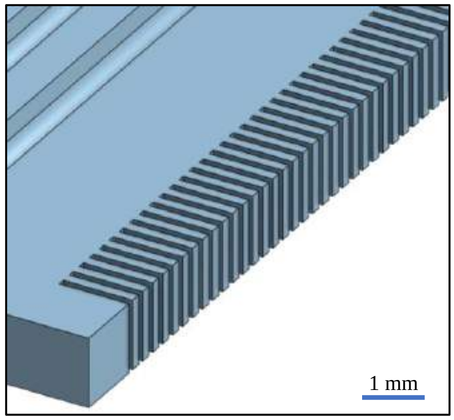

Figure 2.6 *A magnified view of a typical plate showing the sacrificial structures around the edges. These structures are meant to catch excess bronze during infiltration so that the bronze does not flow into and block the channels. The gaps are narrower than the channel diameter, so it is more energy efficient for the bronze to fill these sacrificial gaps before filling the channels.*

The second (sacrificial powder) design is very similar to the first, with slightly different dimensions to accommodate a different bronze control method.

This second design plate design is shown in figure 2.7a. Plates were 1 mm thick, with a base of 30 mm by 20 mm. The channel had the same width, depth, and layout as the other design but was shortened to 31.9 cm long to fit on the smaller plate.

The bottom plate was 4 mm thick and included an infiltrant holder like the other design, but also included a large enclosure or basin to hold the plates and the powder that surrounded them during the infiltration process. The design of a bottom plate is given in Figure 2.7b. Again, the top and bottom plates were made with center holes to allow easier ferrule attachment. An additional lid block was added to raise the height of the stacked plates above that of the base walls. This was done to allow weighted sintering.

Rotational stacking and alignment aspects of the design are the same for both designs. A whole assembly of the second design is shown in figure 2.8. More intermediate plates could be used, only two are shown here.

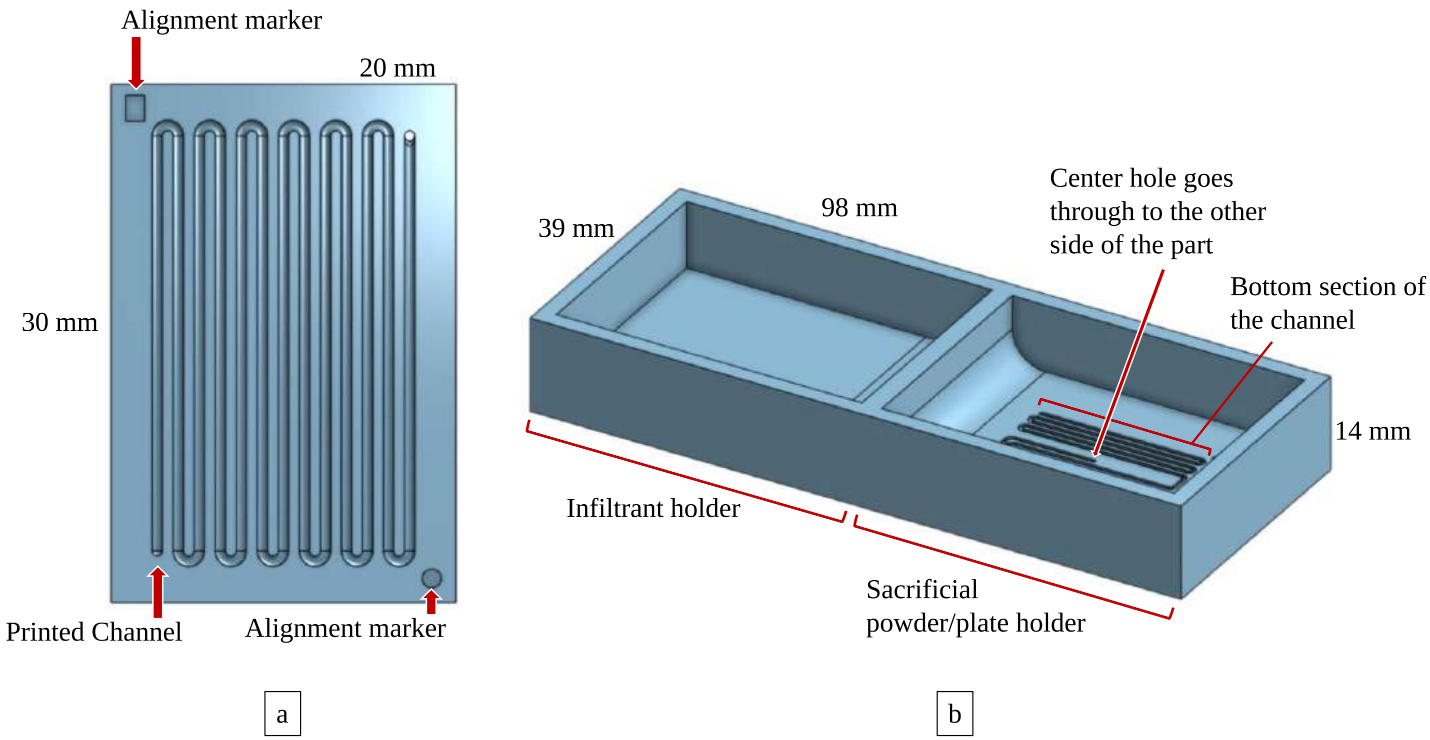

Figure 2.7 *A typical plate in the second sacrificial powder design (a) and the bottom plate (b). The print dimensions of a typical plate are 1 mm x 30 mm x 20 mm with 31.9 cm of channel length. Alignment markers and vertical sections of the channels allow the plates to stack together to create one long channel. Plates do not fit snugly in the plate holder of the base, but rather allow a few millimeters of space to allow a moat of sacrificial powder (not shown). The top and bottom plates have channels that lead out of the center of the plates to allow easier ferrule attachment.*

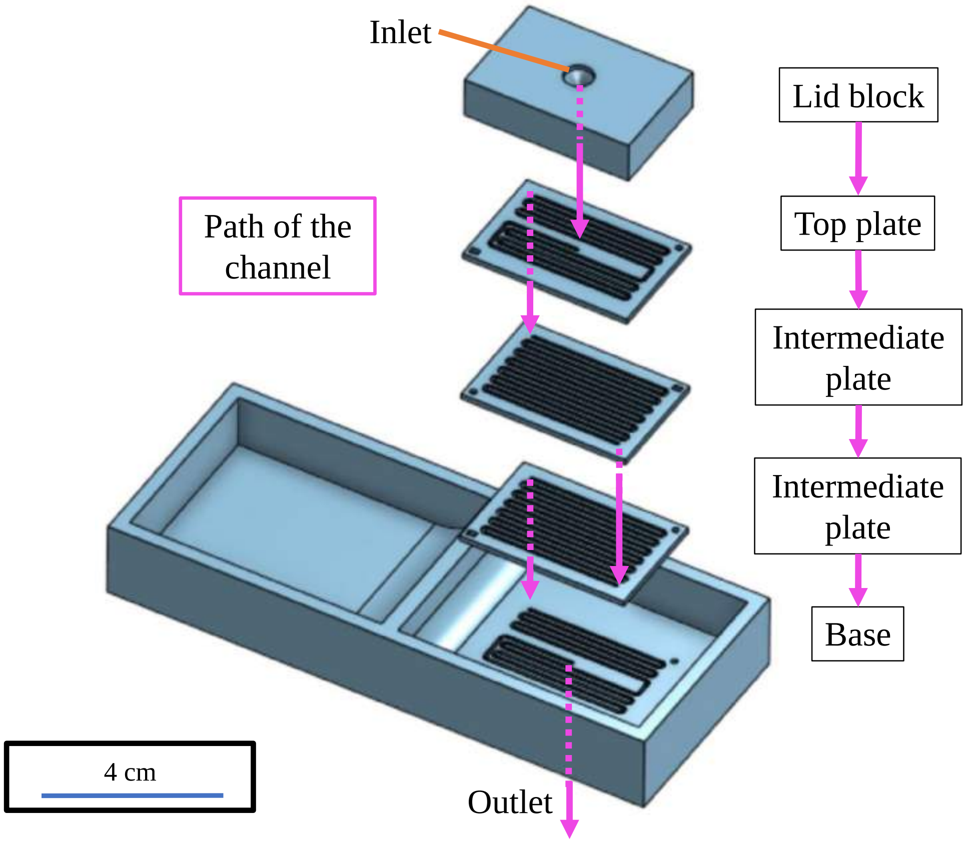

Figure 2.8 *An assembly of the second (sacrificial powder) design of the GC channels. The top plate and base use center exit holes to allow easier attachment to ferrule attachment. Intermediate plates are identical to each other, only alternating by 180 degrees when stacking. More intermediate plates could be used than shown here. A top lid block is used to raise the stacked plate height above that of the base's walls, allowing weighted sintering. The hypothetical flow of gas is illustrated by the arrows.*

2.2 Printing

Parts were printed using an ExOne 3D Binder jet printer and designed using OnShape. The 316L stainless steel powder had an average particle size of 10 µm with the maximum size around 22 µm. After printing and curing, loose powder was removed by an air hose at 40 psi.

A part that has just been removed from the powder bed, also known as a green part, is basically a bunch of powder glued together. This fragile structure must be processed further to make a workable part.

2.3 Sintering

Green parts are fragile and powder easily rubs off of them, which slightly deforms the part. Sintering is a process used to burn out the binder, to harden the structure, to reduce porosity, and to lightly fuse parts together (if multiple parts are sintered in contact with each other). It also results in volumetric shrinkage.

Before being placed in the furnace for sintering, the stackable block structure was assembled together, and a 180 g weight was placed on the channeled plates. The weight visually reduced warping and improved the sealing between plates. The whole assembly was then put into the furnace. Hydrogen was set to flow at 200 standard cubic centimeters per minute (SCCM) and argon at 500 SCCM. The purpose of this atmosphere was to prevent oxidation.

The furnace then heated to 800 ^{o}C and dwelt there for an hour. The temperature increased to 1085 ^{o}C for the first design and 1135 ^{o}C for the second design. Both samples were held at their temperature for twenty minutes. For the last five minutes hydrogen flow was stopped, and argon flow increased to 1800 SCCM to purge the hydrogen. Then the furnace was turned off and the printed sample was pulled to the end of the furnace via a transfer arm. Fans under the ends of the furnace tube, near the endcaps, were used to cool the ends of the furnace to allow faster cooling of the sample before removal. The section of the furnace near the endcaps is significantly cooler than the center. After twenty minutes, the end cap was opened, and the stackable block structure was removed from the furnace. The furnace is shown in figure 2.9.

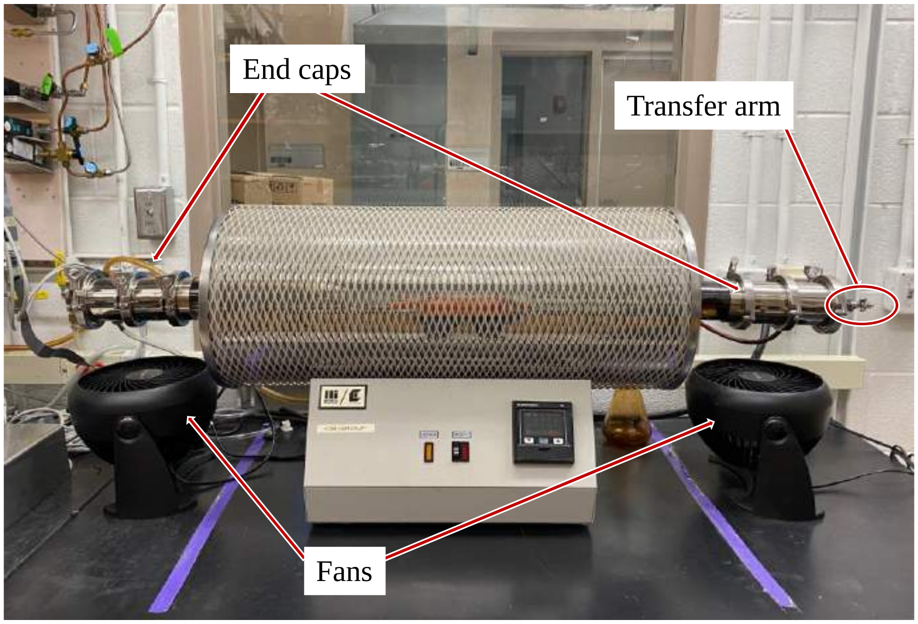

Figure 2.9 *The furnace used in sintering and infiltrating. The transfer arm is mostly inside the furnace and may be pulled (without opening the endcap) to move the sample from the hot center and the cooler endcap.*

2.4 Infiltrating

Infiltration fills unwanted voids in the stainless-steel matrix with bronze, but also may fill channels that we want to keep clear for the gas flow in GC. We cannot simply use the exact amount of bronze needed to reach this precise balance point because there are limits to the accuracy of our measurements and limitations to the assumptions of our model (discussed later). A method for controlling infiltration must be incorporated. We use two different types of buffers: printed sacrificial structures and sacrificial powder.

Infiltrating is a process by which liquid metal flows into a porous structure via capillary action and fills the voids. Although sintering reduces porosity and slightly fuses the plates together, a high void percent remains, and a small stress can break the plates apart. The purpose of infiltration is to further reduce porosity and improve the seal between the plates. Pores and gaps between plates are undesirable because we want to flow gases through these channels. If a portion of the gas becomes trapped in a pore, the resulting analysis of the sample would be inaccurate, and may compromise additional samples. If gas escapes through a crack, the analysis is likewise inaccurate. If gas is allowed to flow through the printed matrix and is not confined to only travel through the channels, the shortcuts would ruin the separation of the gas into its unique components and render the machine useless.

During the infiltration, the whole assembly is heated to a temperature higher than the melting point of the bronze infiltrant, but lower than that of the stainless-steel structural frame. While being held at that temperature, the liquid bronze flows thorough the frame via capillary action and fills the structure's voids. To minimize surface energy, the infiltrant prefers to fill smaller pores before larger ones. Thus, the small voids in the stacked structure are filled first, then the larger gaps between plates are filled next. The voids and gaps between plates must be filled to prevent gases from escaping the GC channel. The infiltration process is illustrated in figure 2.10. Although the figure uses sacrificial powder in reference to the second sample design, the concept is the same for printed sacrificial structures.

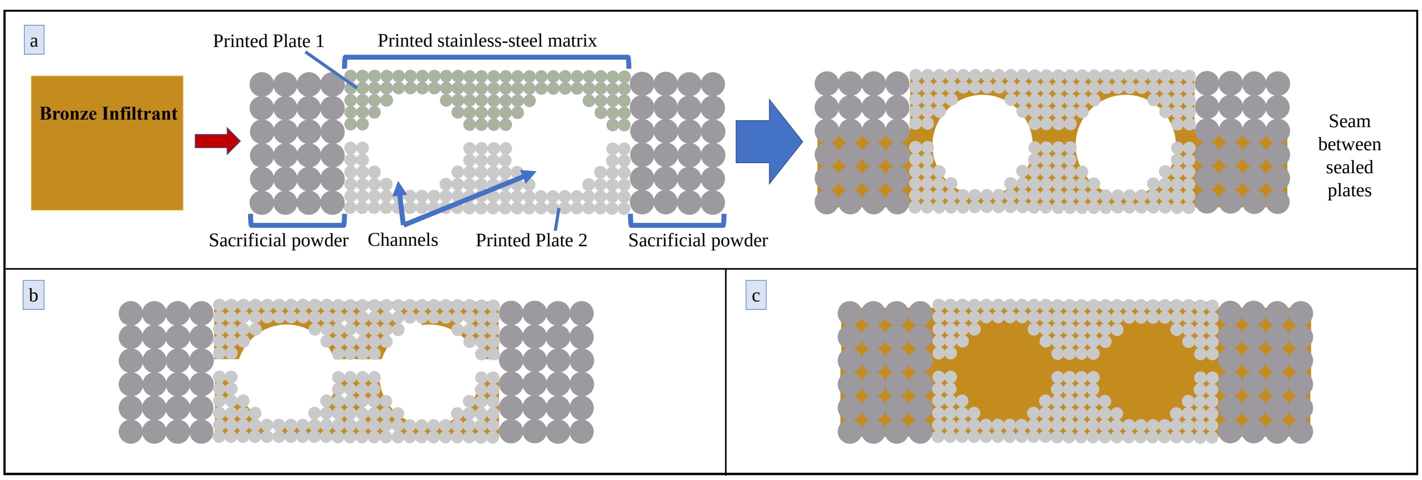

__Figure 2.10__ Infiltration process. Successful infiltration (a). The bronze infiltrant flows into the printed stainless-steel matrix via capillary action, filling smaller void spaces before larger ones. The metal infiltrant fills interstitial pores in the printed matrix, partially fills pores in the sacrificial powder, and does not fill the GC channels. The bronze also seals the two plates together. Failed infiltrations are also shown. Too little infiltrant (b) doesn't seal the plates together and leaves large pores in the matrix. There would not be any infiltrant in the sacrificial powder. Too much infiltration (c) fills everything including the channels.

The bronze needed for infiltration was calculated using the following equation:

$$M_b = \rho_b V_p (1 - \frac{M_m}{V_p \rho_s})$$

M_b refers to the mass of the bronze needed for the infiltration, while M_m is the measured mass of the sintered assembly. The density of liquid bronze is represented by ρ_b, and ρ_s is that of stainless steel. V_p is the volume of the sintered piece, excluding empty spaces that were designed into the part. V_p is calculated by using the CAD volume measurement and multiplying by a volumetric shrinkage factor. The shrinkage is calculated by measuring the ratio of the post-sintered base piece to the pre-sintered base piece along the three dimensions.

The equation above assumes one hundred percent void filling, a similar thermal expansion for the stainless steel and bronze, and a perfect print. These assumptions are not completely true and so a margin of error must be accounted for. Too little bronze would fail to fill the voids, while too much bronze would block the channels. Excess bronze must flow somewhere, but the channel cannot be blocked. The purpose of the sacrificial structures and sacrificial powder is to divert excess bronze. Sacrificial structures were designed with gaps larger than gaps between plates (which we want to be filled) and smaller than the diameter of the channels (which we do not want to be filled). These sacrificial structures are the ridges on the edges of the plates (see figure 2.6).

The size of the sacrificial powder was chosen with the same constraints. The sacrificial powder works in the same way as the structures. The large-grained (100 mesh) powder leaves space between particles that are larger than the pores of the printed matrix and smaller than the channel diameter. An advantage of the powder is that we can have more sacrificial pores surrounding the plates and these pores can be smaller than what we can print.

To infiltrate our samples, the bronze (c90700) powder was poured into the infiltrant holder, and the structure was placed into the furnace. Hydrogen flowed at 200 SCCM and argon at 500 SCCM. These gases prevent oxidation. For the first design, the furnace was heated to 1085 ^{o}C and held there for forty minutes. For the second design, the furnace was heated to 1135 ^{o}C and held there for two hours. For the last five minutes of both processes, hydrogen flow was turned off and argon flowed at 2800 SCCM to purge the hydrogen. The fans at the ends of the furnace were turned on and the sample was pulled to the end of the furnace to begin cooling. The first design samples were removed after 25 minutes. The second design samples were removed after 15 minutes. Samples were rapidly cooled by being taken from the furnace while still at a high temperature. This reduced the likelihood of bronze crystallization, which would have resulted in crystals blocking the channel.

2.5 Imaging

To see the internal structure of the channels, we had to mill the samples and inspect the parts under a microscope. We looked for debris in the channels, infiltrant overflow in the channels, bronze migration, and crystallization. We wanted to avoid the occurrence of these features. We also looked for the desirable features: fused plates and infiltrant overflow in the sacrificial structures. For most of the imaging, we used the Olympus microscope and Moment Macro lens.

The sample was milled with a tungsten carbide ½" end mill at about 1080 rpm and a slow, hand-cranked feed. The side of the mill was used in a climb cut. Cuts were usually 15/1000 inches (380 μm) deep.

Chapter 3 RESULTS AND DISCUSSION

3.1 Printing

The printing method had limitations that we were able to design around. The plate design had to allow for powder removal, variability in bronze infiltration, layering ability, alignment, and channel uniformity. The extra powder from the print bed could easily be removed by the air hose and no extra powder remained in the printed channels. While most of the sacrificial structures were wholly cleared, a few sacrificial structures only partially cleared. There was minor variability in printing these parts only a few hundred microns across. After curing, the powder of the green pieces is loose, so features are easily broken. This sometimes degraded the alignment features and resulted in poorer alignment and broken sacrificial structures. The print orientation affected the quality of the print. For example, the small slits of the sacrificial structure were more accurately printed if parallel to the printer bed.

3.2 Sintering

Sintering hardened the parts, mildly sealed the pieces together, and resulted in some shrinkage. The plates stuck together but came apart when under stress (due to milling, cutting, etc.). Infiltration was needed to seal the plates together enough – to truly seal the channels running through each individual plate into one long channel and to withstand the forces required for imaging.

The sintering process changed the sample dimensions. Volumetric shrinkage during sintering was about 18%. Samples had to cool sufficiently before being removed from the furnace to avoid oxidation. A sintered sample of the first design with bronze powder in the holder (ready for infiltration) is shown in figure 3.1a. The same sample after infiltration is shown in figure 3.1b. Examples of sintered (pre-infiltration) and post-infiltration samples of the second design are shown in figure 3.2.

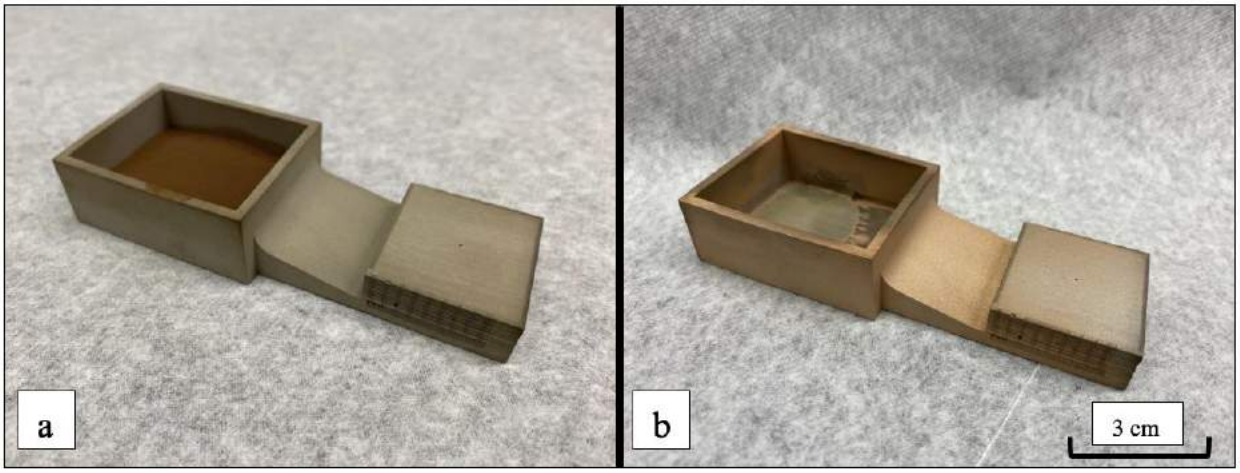

__Figure 3.1__ The assembled structure (first design: sacrificial structures) after sintering with bronze powder in the infiltrant holder (a) and the structure after infiltration (b).

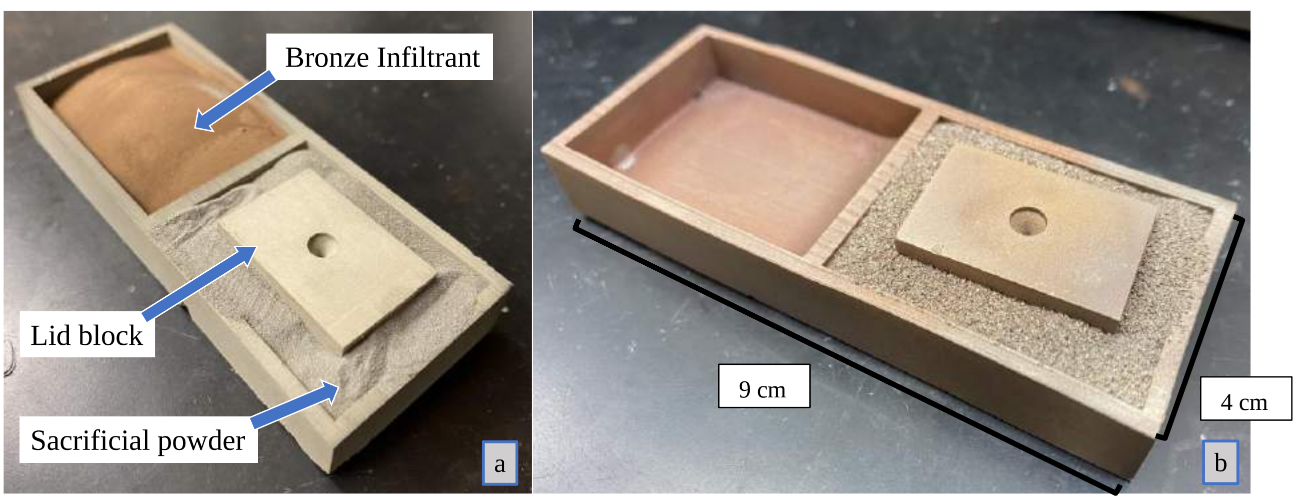

__Figure 3.2__ An example of the assembled structure (second design: sacrificial powder) after sintering with bronze powder in the infiltrant holder (a) and the structure after infiltration (b). These are two separate samples and different points in the manufacturing process.

3.3.1 Infiltrating the Sacrificial Structure Design

Infiltrating worked as desired in some respects, but not in others. The two designs had different levels of success.

We expected and desired excess bronze to fill sacrificial structures instead of filling channels, but this was not the case. Despite plenty of sacrificial space still unfilled (figure 3.3), some sections of the channels did fill (figure 3.4). As desired, bronze sealed the plates firmly together (figure 3.5). Not all bronze infiltrated into the stainless steel. A small amount of bronze sometimes remained in the holder or pooled along the edges of the structure. Placing runners between the infiltrant holder and stainless-steel plates allowed more controlled infiltration. However, bronze infiltrant was unable to migrate through cracked runners and could not fully absorb past an oxidized layer on the steel.

Through infiltration, the pores in the stainless-steel structure are filled with bronze. However, this process must be carefully controlled. If too little bronze is present, not all the voids will fill. If too much bronze is present, it will seep out of the framework and obscure details. Excess bronze may block or restrict the channels. By including sacrificial structures on the channeled block, we allow excess bronze to flow into midsized voids instead of filling the larger openings of the channels.

The infiltration time had to be long enough for the liquid bronze to reach equilibrium. The mixing of metals in liquid (bronze) and semi-liquid state (steel) may be able to distort small geometries on the plates. The structure had to cool rapidly to avoid bronze crystallization, which could block the channels.

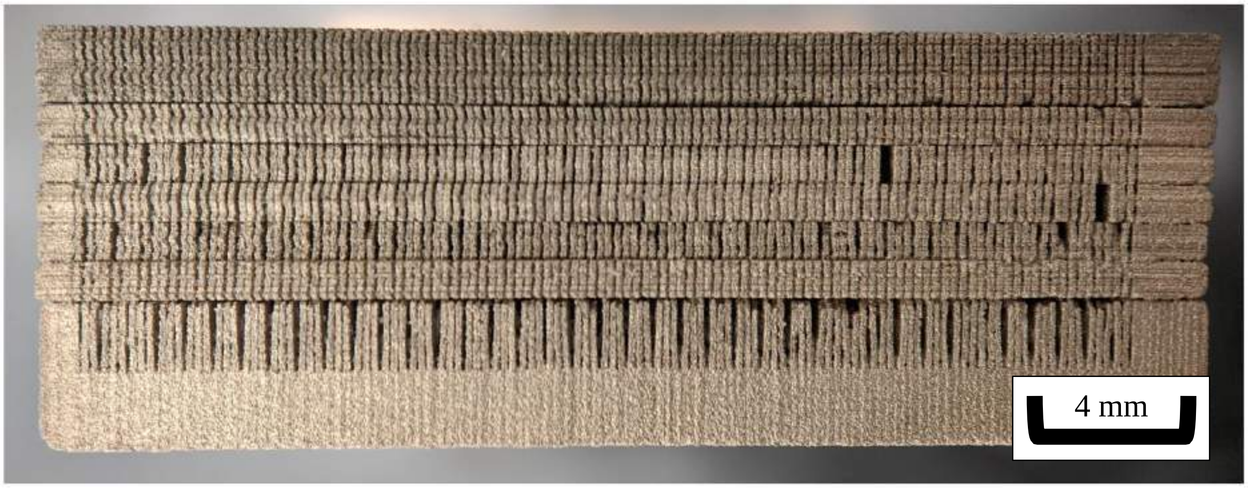

Figure 3.3 *Side view of an infiltrated assembly with the first design. Some gaps between the sacrificial structures were filled with bronze, some were not. Large gaps in the pattern indicate where sacrificial structures broke off during pre-sintered handling. This sample had partial filling of channels. The groupings of slitted structures (especially visible in the bottom layer) may be due to printing resolution.*

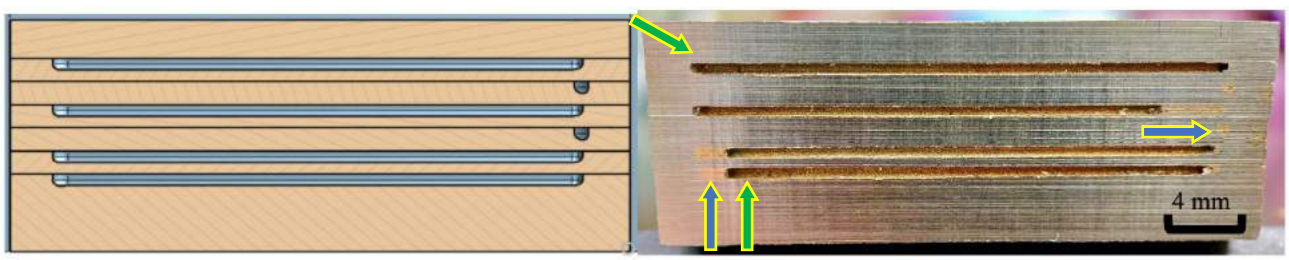

Figure 3.4 *CAD assembly (left) and infiltrated sample (right) both cut at 3.81 mm from the edge opposite the holder. Not every layer shows a channel due to the offset in the plate design and the alternating 180 degree rotation of the plates. The rough bronze-colored streaks show unfilled channels (some examples indicated with blue arrows) while the smooth bronze-colored sections show filled channels (some examples indicated with green arrows). The channels here are mostly unfilled, but there is some filling, on the sides of the block. Image on the right is taken by a Moment Macrolens and was filtered to show better contrast.*

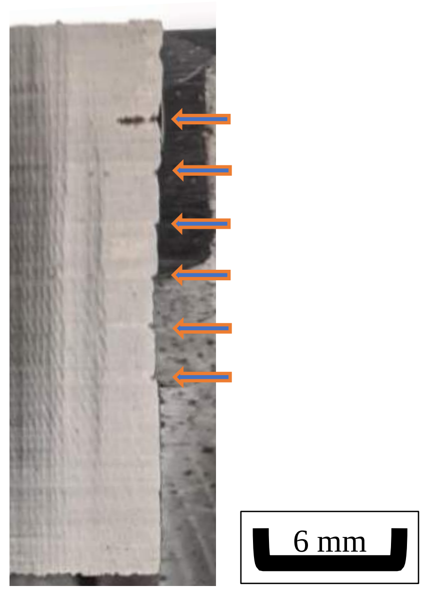

Figure 3.5 *Plate Sealing. The locations of the seams between plates are indicated with arrows. These areas are slightly indented and bronze-colored compared to the surrounding plates.*

3.3.2 Infiltrating the Sacrificial Powder Design

The sacrificial powder proved to be a better bronze control than the printed sacrificial slits. This is likely due to the more abundant pores available for the bronze to fill as well as more optimal pore sizes. According to our model, infiltrant will fill the smallest pores first: those within the printed matrix, then the next size up: the gap between plates, then the pores within the loose powder moat, then the channels themselves. The pores within the moat act as a buffer between what we do want filled (the pores in the matrix and the gap between plates) and what we do not (the channels themselves). The more sacrificial pores that there are, the better the buffer is. The better the relative size of the sacrificial pore fits in the filling sequence, the better the buffer is as well. This allows more flexibility in the exact amount of bronze used and allows for minor errors in measurements and assumptions.

The infiltrant filled the interstitial pores in the printed powder, reducing the porosity of the structure. The separate plates sealed together, forming one continuous channel. The seams between plates still showed some small pores, indicated by the blue arrows in figure 3.6a. Some pores remained in the sacrificial powder, as expected (figure 3.6b). The channel remained clear of infiltrant, allowing necessary gas flow. The bronze/steel composition of the infiltrated part is shown in Figure 3.7.

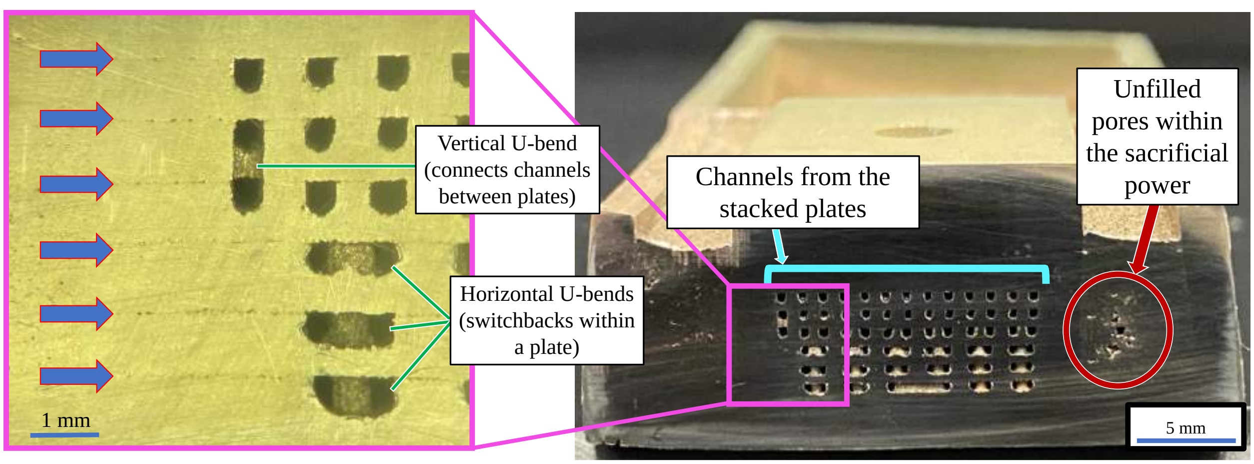

Figure 3.6 *A polished cross section of the infiltrated part (second design). The image to the left is an inset of the image to the right. This assembly consisted of a base, 5 intermediate plates, and a lid block. The cross section is not edge-on, but tilted 5 degrees, and thus shows horizontal U-bends in the bottom three rows of channels but not in the upper three.*

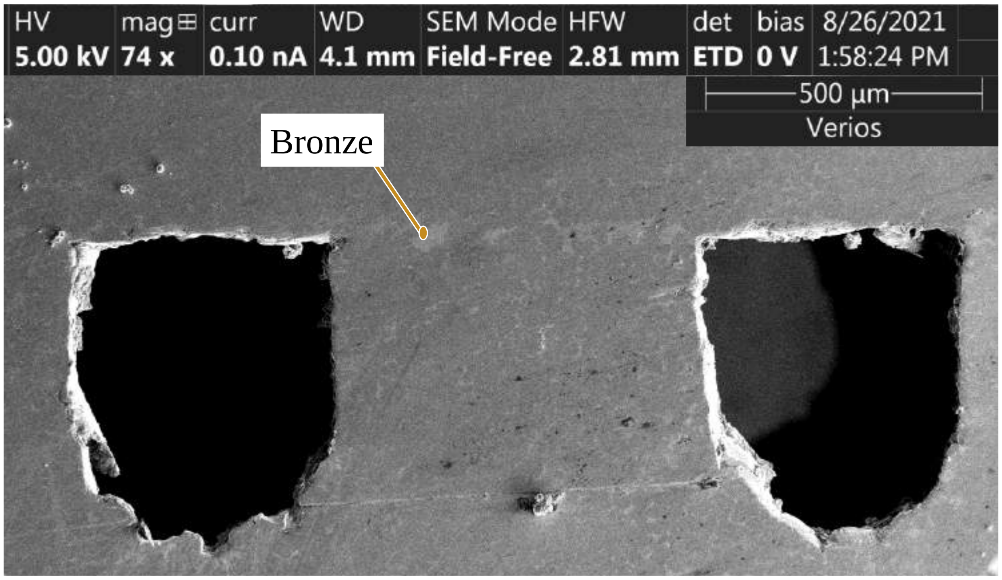

Figure 3.7 *An SEM image of two cross-sectioned channels. The majority of the structural frame is made up of fine grain stainless steel particles (dark gray color). Bronze (lighter gray) fills in the gaps between these grains. Larger regions of bronze are visible at the seam; one such spot is indicated in the figure.*

3.4 Imaging

To image and evaluate the channels, the samples had to be milled and occasionally polished. The mill would sometimes push metal into the channels, making them appear blocked when they were not. This was not an issue because the blocking from milling and the blocking from bronze have different textures, colors, and ductility. Inherent structural features from the manufacturing process could be told apart from the features of the imaging process. Some left over stainless steel was occasionally bent by hand and torn from the edges of the channels, resulting in different channel outlines than the sample originally had from the manufacturing process.

3.5 Discussion/Evaluation

Our research led to some desirable results but is not yet complete. A moat of sacrificial powder was more successful than printed sacrificial slits. We could see the bronze-filled pores of the matrix in polished samples. Some voids remained in the sacrificial powder, showing that is it an effective buffer. We were able to successfully seal the plates while leaving channels cleared, creating a single 3D channel about 1.7 m long using the second design.

Infiltration was needed to do the sealing because the sintering temperature was not high enough to fuse the separate steel plates together sufficiently. Bronze infiltration was also necessary to fill voids inherent in 3D printed pieces. The finished channels were not very smooth, partially due to the printing and partially due to the infiltration. This is a potential issue for gas chromatography, but the roughness was found to be within the acceptable limit.

From the beginning, our research was not quite in line with μGC standard. Industry standard of μGC systems is about 250 μm diameter channels. The channels made in this study were 500 μm in diameter. This is somewhat larger than standard, but within a reasonable range.

We conclude that 3D printing and infiltration is a feasible method to make channels suitable for μGC, but more research is needed. Further work understanding the infiltration process, higher furnace temperatures, and different sizes of sacrificial powder may lead to more consistent and desirable results. There is a high potential for longer channels with smaller diameters to be made with this process. Plate geometries and channel geometries in our study were adjusted, but not optimized. Higher channel density per plate could be achieved with further design improvements. Alignment could be improved, a main issue being that the protruding alignment markers are very small and are easily rubbed off of the green part. Further research is also needed to be able to connect the channels to other parts of a gas chromatography system (injection port, mass spectrometer, etc.).

Bibliography

[1] Azzouz, F. Marty and T. Bourouina, "Recent advances in micro-gas chromatography — The opportunities and the challenges," 2017 Symposium on Design, Test, Integration and Packaging of MEMS/MOEMS (DTIP), Bordeaux, 2017, pp. 1-5, doi: 10.1109/DTIP.2017.7984485.

[2] Ghosh, Ghosh, Abhijit, et al. "Microchip Gas Chromatography Columns, Interfacing and Performance." Talanta, vol. 188, 2018, pp. 463–492., doi:10.1016/j.talanta.2018.04.088.

[3] Radadia, A. D.; Morgan, R. D.; Masel, R. I.; Shannon, M. A. Anal. Chem. 2009, 81, 3471−3477.

[4] Cordero, Zachary C., Siddel, Derek H., Peter, William H., and Elliott, Amelia M. Strengthening of ferrous binder jet 3D printed components through bronze infiltration. Netherlands: N. p., 2017. Web. doi:10.1016/j.addma.2017.03.011.

[5] Abdulhameed O, Al-Ahmari A, Ameen W, Mian SH. Additive manufacturing: Challenges, trends, and applications. Advances in Mechanical Engineering. February 2019. doi:10.1177/1687814018822880

[6] Iwaya, Takamitsu, et al. "Development of High Precision Metal Micro-Electro-Mechanical-Systems Column for Portable Surface Acoustic Wave Gas Chromatograph." Japanese Journal of Applied Physics, vol. 51, 2012, doi:10.1143/jjap.51.07gc24.

[7] Mirzababaei, S.; Pasebani, S. A Review on Binder Jet Additive Manufacturing of 316L Stainless Steel. J. Manuf. Mater. Process. 2019, 3, 82. https://doi.org/10.3390/jmmp3030082

[8] Radadia, Adarsh D. et al. "The effect of microcolumn geometry on the performance of micro-gas chromatography columns for chip scale gas analyzers." Sensors and Actuators B-chemical 150 (2010): 456-464.

[9] Regmi, Bishnu P., and Masoud Agah. "Micro Gas Chromatography: An Overview of Critical Components and Their Integration." Analytical Chemistry, vol. 90, no. 22, 2018, pp. 13133–13150., doi:10.1021/acs.analchem.8b01461.

Index